# Armed Services Technical Information Agency

## AD 43390

# UNCLASSIFIED

Technical Report No. 1

Contract N6 ori 071 (54)

CRYSTAL PERFECTION IN ALUMINUM SINGLE CRYSTALS

T. S. Noggle and J. S. Koehler

Department of Physics

University of Illinois

Urbana, Illinois

September, 1954

## ABSTRACT

A high resolution x-ray diffraction technique has been employed on annealed single crystals of aluminum in order to arrive at an estimate of dislocation densities and distributions. This work indicates that in annealed aluminum crystals the majority of the dislocations are present in an essentially random array with densities of the order of $10^6$ lines/cm$^2$. Small angle boundaries, which are commonly present, contribute about $10^4$ to $10^5$ lines/cm$^2$ to the dislocation density. Comparison of crystals obtained by growth from the melt and by recrystallization indicates that there are no basic differences in the degree of crystal perfection obtained using the two methods of growth.

Crystal Perfection In Aluminum Single Crystals

T. S. Noggle and J. S. Koehler

University of Illinois, Urbana, Illinois

## INTRODUCTION

It is generally accepted at the present time that a
type of crystal imperfection called a dislocation plays a very
important role in determining many of the properties of crystals.
The influence of dislocations on the properties of crystals
arises as a result of the inherent properties of a dislocation
and its interaction with other dislocations or other types of
lattice defects.  Despite the recognized importance of the role
of dislocations on properties such as mechanical strength,
damping and electrical resistance, there has been but little
work done toward obtaining direct estimates of dislocation distri-
butions and densities.  This state of affairs is primarily due
to the lack of completely satisfactory methods of measuring
dislocation densities and distributions.  Recently developed
x-ray diffraction techniques[1][2][3] offer hope of improving
this situation, and as applied particularly to metal crystals,
are capable of giving semi-quantitative estimates of dislocation
densities.  In addition these methods can detect the presence of
and measure the magnitude of a particular type of dislocation
distribution commonly referred to as a small angle boundary.
Information of this kind is of importance in the interpretation
of physical behavior in terms of dislocation theory.

The present investigation was carried out to assess the
possibilities of using x-ray measurements to determine the
dislocation structure of reasonably well annealed aluminum single
crystals. In addition, single crystals of aluminum obtained by
different growing methods were examined to ascertain if there
were measurable differences in the degree of crystal perfection
and if any basic differences in the type or distribution of the
imperfections could be detected.

## GENERAL CONSIDERATIONS

X-ray diffraction theory predicts that reflection of
x-rays from a set of lattice planes in a perfect crystal should
occur over an angular range of a few seconds of arc. In
practice, it is found that most crystals give reflections over
an angular range in excess of one minute. This spread in the
angular range can be interpreted in terms of a mosaic block
structure in which the angular range of orientations is given
by the spread of the reflection. This concept of a mosaic
structure was initially introduced by Darwin[4] to account for
the observed intensities of reflections from real crystals.
Theory indicated that the observed intensities could be accounted
for by a mosaic block size of mean diameter $10^{-4}$ to $10^{-5}$ cm.
This mosaic structure can be interpreted in terms of dislocation
distributions in which the boundaries between the blocks are
defined by dislocations, and for the block sizes above would give
dislocation densities of $10^8$ to $10^{10}$ lines/cm$^2$.

In addition to the spread in the reflection angle which arises from the tilting of the blocks, contributions to the angular range of the reflections should arise due to the size of the mosaic blocks and from the strains associated with the presence of dislocations.

Cottrell[5] discusses the interpretation of the spread of x-ray reflections in terms of possible dislocation models for the case of tilting of the mosaic blocks. The type of model that he indicates should give the most reliable estimates of dislocation densities consists of a linear array of blocks of mean size l, each block tilted by the angle $\alpha$ relative to its neighbors, $\alpha$ being randomly positive or negative. For this case, the probable angular deviation $\epsilon$ between two points in the crystal separated by the distance L is given by:

$$\epsilon = \alpha\sqrt{\frac{L}{l}} \tag{1}$$

Assuming that the angle $\alpha$ is due to a single dislocation in the block boundary, the probable angular deviation is related to the dislocation density by the relation:

$$\epsilon = b\,\rho^{3/4}\sqrt{L} \tag{2}$$

where b is the Buerger's vector of a dislocation and $\rho$ is the dislocation density in lines/cm$^2$.

Extension of this theory to the two-dimensional case and to a derivation of the distribution function of the one-dimensional model leads to results similar to equation (2) in that the mean

square deviation increases with increasing sample size. The
conclusion from this is that if dislocation distributions are
essentially random, then the expected angular deviations will
increase with increases in the crystal size or of the region
investigated. This point can be checked experimentally. In
addition, the tilting block model indicates that this source of
angular spread of the reflections is independent of the reflection
angle and offers the possibility of sorting out its contributions
from other sources of line broadening which are dependent on the
diffraction angle.

The particle size broadening equation gives the increase
in the angular spread of the reflection associated with the size
of the coherently reflecting region.[6] This relation is:

$$w - w_0 = \frac{0.9\lambda}{1 \cos \theta} \tag{3}$$

w = experimental line width

$w_0$ = instrumental line width

λ = wave length of x-rays reflected by the crystal

θ = Bragg angle

1 = mean particle size

This equation predicts an increase in the line width due to
decrease in the particle size. For a given system (λ,1 constant)
the line width observed will vary as a function of secant θ. In
practice, the application of this relationship to the interpretation
of experimental data requires accurate knowledge of the instrumental
line widths—particularly in the case of annealed crystals where 1

is relatively large and the expected changes in line width are small.

The influence of lattice strains on the angular range of the reflections arises due to the change in the diffraction angle with changes in the interplanar spacing. The shift in the reflection angle is given by:

$$\Delta\theta = -\,\varepsilon\,\tan\theta \tag{4}$$

where $\varepsilon$ = strain, $\theta$ = diffraction angle.

A uniform strain will simply produce a shift in the diffraction angle without any change in the angular range of the reflection. However, a non-uniform strain will give a contribution to the line width due to variation in $\varepsilon$. The line width increase $\Delta w$ due to a range of strain $\Delta\varepsilon$ is given by:

$$\Delta w = \Delta\varepsilon\,\tan\theta \tag{5}$$

In order to relate equation (5) to dislocation theory, the mean strain due to dislocations in a crystal can be estimated by averaging the strain due to a single dislocation over the region surrounding the dislocation to points midway between adjacent dislocations. This type of calculation can be carried out for edge type dislocations and gives:

$$\sqrt{\overline{\varepsilon^2}} = \frac{b}{R}\sqrt{\log\frac{R}{r_o}} \tag{6}$$

where: $\varepsilon^2$ = the mean square tensile or compressive strain.

b = the Buerger's vector of a dislocation.

R = the radius of the region occupied by the dislocation

$r_o$ = the radius of a region around the core of the
dislocation in which equation (6) is not applicable
due to failure of the elasticity equations from
which (6) is derived in the region of large strains
near the center of the dislocation. This region
extends several atomic dimensions around the dislo-
cation and is given a value of $6 \times 10^{-8}$ cm in
subsequent calculations.

Equation (5) gives the mean tensile strain in the region below a
positive edge dislocation, or the mean compressive strain in the
region above the dislocation. Thus, the range of strain will be
twice the mean strain. Taking this into account, and also that
$R \simeq \dfrac{1}{2}$ we get:

$$\Delta w = 4 \, \rho^{1/2} \sqrt{\log \frac{1}{2 r_o \rho^{1/2}}} \cdot \tan \theta \qquad (7)$$

The increase in line width predicted by this equation would be due
only to edge type dislocations since screw type dislocations
introduce no dilation of the lattice.[4b]

In addition to the sources of line broadening discussed
above, small angle boundaries are usually present in metal crystals
and are detected readily by high angular resolution x-ray diffraction
techniques. They are observed in an x-ray reflection as a displace-
ment between one portion of the reflection and another. The angle
associated with this displacement is a direct measure of the angular
misorientation occuring at the boundary. The simplest type of
boundary that can be constructed using dislocations, consists of a

sheet of parallel edge type dislocations of the same sign with a mean spacing h between the dislocations. For small angular misorientations, the angle of tilt of the boundary is: $\alpha = \frac{b}{h}$   (8) where: $\alpha$ = tilt angle of boundary    b = Buergers vector of the dislocations

High resolution x-ray diffraction methods have been applied to metal single crystals by several investigators, and their results have indicated that a higher degree of crystal perfection than heretofore expected sometimes exists in carefully handled single crystals obtained by recrystallization. Guinier and Tennevin[1] using a focusing Laue method, reported a maximum disorientation in certain aluminum specimens of less than 30 seconds of arc over regions involving about 30 $mm^3$. In terms of the tilting block model for estimating dislocation densities (equation 2), this gives a dislocation density of $\rho = 2.3 \times 10^5$ lines/cm. Lambot, Vassamillet, and Dejace[2] employing a method similar to that used in the present investigation, reported for Al and Fe single crystals a maximum disorientation of 50 seconds of arc. This corresponds to a dislocation density of about $7.5 \times 10^6$ lines/$cm^2$. Gay, Hirsch and Kelly[3] using a micro beam technique, report the upper limit for the dislocation densities in annealed aluminum as $3 \times 10^8$ lines/$cm^2$. In that their work was carried out on polycrystalline material, it is not clear that their results are comparable to results obtained on single crystals.

## EXPERIMENTAL METHODS

High purity aluminum single crystal specimens were prepared in the form of square tensile specimens 1 cm square by 6 cm long in the reduced section of the bars. One group of specimens was prepared by the strain-anneal method of Schwope, Shober, and Jackson[7]. The other group of specimens were prepared by the " soft mold" method[8]. Both groups of specimens were prepared from the same bars of hi-purity aluminum $(99.99^{+}\%$ Al)[*].

After the appropriate crystal growing cycles had been carried out, the specimens were etched in a macroetch solution[9] which was capable of showing orientation differences of about $1/2^{o}$. The presence or absence of visible disorientations on the etched specimens was used as a criterion for sorting them into satisfactory and unsatisfactory categories. Most of the specimens processed by the strain-anneal method required an anneal of 20 - 50 hours at $650^{o}C$ to eliminate isolated grains that remained after the growing cycle. The yield of satisfactory specimens was about the same for each method, being slightly better than 50 per cent.

## X-RAY METHODS

The x-ray method used was essentially the same as that described by Lambot, Vassamillet, and Dejace[2]. Our experimental set-up is indicated schematically in figure 1. It employed a G.E. CA7, copper target, x-ray tube with the beam taken from the line focus port at about $4^{o}$ to the plane of the target. A bent crystal

*Supplied by Aluminum Research Laboratories, Aluminum Company of America.

monochromator intercepted this beam and reflected a monochromatic beam which was convergent in the horizontal plane and divergent in the vertical plane. When properly adjusted the monochromator gave a fine line focus in which the Cu - Ka doublet was cleanly resolved. The charactersitics of the beam obtained from the monochromator are listed in Table 1.

Specimens were held in a goniometer which could be adjusted so that the plane of the surface being investigated coincided with the vertical axis of rotation of the goniometer which in turn had been adjusted to coincide with the monochromator focus. The orienting of specimens to obtain reflections was facilitated by prior knowledge of the orientation obtained by the back reflection method.

In the adjusting of the monochromator, it was found convenient to employ a long focal length microscope to observe the focus on a fluorescent screen. Use of this method improved the speed and reproducibility of adjustment over that of the photographic method. In addition, the use of a portable Geiger counter to detect and locate the reflection from the specimen facilitated the accurate adjustment of the specimen for maximum intensity of reflection.

Reflections were registered on film at a distance of one meter from the specimen. Exposure times varied from 10 minutes for the (111) reflection from aluminum to about 2 hours for the (333) reflection. The films were scanned on a L and N microphotometer and line widths measured at one-half the maximum film

density. Figure 2 shows several reflections obtained by this method. Figure 3 shows a typical microphotometer record obtained from an aluminum specimen.

Aperturing of the incident beam was carried out to test the predictions of the theory based on the tilting block model. This was accomplished by inserting lead slits into the path of the incident beam at a point about 1 um. in front of the specimen. By this means the vertical height of the beam at the specimen could be varied from 0.1 mm to the full beam height without disturbing the monochromator or specimen adjustments and without sensibly affecting the angular aperture of the incident beam. These aperturing tests were carried out on aluminum specimen D, grown from the melt, which fortuitously combined the attributes of a good degree of crystal perfection andan orientation such that the (111) reflection could be obtained under nearly optimum experimental conditions. In addition, similar tests were carried out on a quartz crystal using the $(2\bar{1}0)$ reflection. This reflection occurs at a Bragg angle very nearly the same as the (111) reflection from aluminum.

In order to determine the angular dependence of the line widths, a number of reflections which covered the range of reflection angles possible were obtained from one face of aluminum specimen D. All reflections were obtained from the same region of the specimen. Three reflections covering about the same angular range were obtained from the quartz crystal for comparison.

A survey was carried out on a number of aluminum specimens

for comparison between the strain-anneal and the melt-grown speci-
mens. Reflections were obtained from each of the four faces of a
specimen, usually near the central region along the length of the
specimen. Six specimens, three of the strain-anneal and three of
the melt-grown, were checked at two different positions separated
by about 3 cm along the length of the specimen. No significant
differences in the degree of crystal perfection was observed
between the top and bottom regions, so the balance of the specimens
were examined only near the center.

## RESULTS

Aperturing Tests: The results of the aperturing tests on
line widths are tabulated in Table 2 and summarized graphically
in figure 4. The interpretation of the behavior observed is
reasonably direct, but requires some understanding of the geometry
of the experiment.

If all possible paths are considered by which a ray can
arrive at and be reflected from a point on the specimen which is
centrally located with respect to one of the lines in the focus,
it is found that there is a vertical angular range (vertical
angular aperture) of about $3/4^\circ$ over which this can occur. As a
result, the reflection from this point is registered on the film
as a short arc whose vertical length corresponds to about $3/4^\circ$ and
whose horizontal width is determined by the material giving the
reflection and by the spectral range present in the x-ray beam.
Points on the specimen which are close enough to each other will

give reflections which overlap and reinforce the intensity at the film. This condition varies with the vertical position along the focus. For reflection from points above and below the midpoint of the focus, the vertical angular aperture is reduced, and the direction of the ray producing the center of the reflected arc will no longer be horizontal, but will have a small vertical inclination. At the extremities, the vertical aperture is very small and the mean paths are inclined at about $2^\circ$ to the horizontal. This can be seen in the reflections shown in figure 2 in which the lines taper off in intensity at either end due to the reduction of the vertical aperture at the top and bottom ends of the focus. The central portions of the lines which are uniform in intensity are from the central region of the focus where changes in the vertical aperture and the inclination of the mean path are small. This region of uniform intensity in the reflection is estimated to correspond to the center 4 mm. of the focus, and this is the region in which the slits were used to define the beam height. In this portion of the reflection, the experimental line width is determined by instrumental contributions[*] and by the angular variations present in the material in an area defined by the focal width and about 1 mm. of length along the focus.

Inserting a slit to define the beam height at the specimen will not affect the line width in the central part of the reflection

[*] The instrumental contributions to the widths of reflections obtained with our experimental set-up have been treated in some detail by Lambot, Vassamillet, and Dejace.[2] Except for the contribution due to spectral width, the instrumental contributions for the reflections observed in the aperturing tests are quite small and lead to no serious errors if neglected.

until the slit height becomes less than the maximum separation distance of points giving overlapping reflections. For slits less than this critical size, the area contributing to the reflection is reduced. In the aperturing experiments, this critical size corresponds to about 1 mm., and for slits in the range of 0.5 to 1.0 mm the variation in the line widths qualitatively follows the behavior predicted by equation (2). Below 0.5 mm, the gradual upturn and sharp increase in the line width is believed due to scattering of the incident beam at the edges of the slit. This factor would become relatively more pronounced with decreasing slit heights as is evident in the large values of the line widths for the 0.1 mm slit.

Due to the limited range of slit sizes for which the line widths vary, it is not possible to check in detail whether these changes follow the square root relation of equation (2). A rough check can be made from the ratio of the line widths for the 1.0 mm and 0.5 mm slit sizes. This ratio is 1.46 for the aluminum specimen and 1.40 for the quartz. The ratio expected from equation (3) is 1.41. The agreement between experiment and the tilting block model theory is surprisingly good, particularly in view of serious doubts that arise as to the applicability of a theory based on a one-dimensional model to a three-dimensional (or at best quasi two-dimensional) system. The important result of these measurements is that the behavior observed is qualitatively consistent with the behavior expected from a system containing a random dislocation distribution.

Further consideration of the applicability of equation (2) to observations made during this investigation reveal some features which are of interest. If we use equation (2) to calculate probable angular deviations for widely separated points in the crystal (L = 1 cm) for dislocation densities in the range of $10^6$ lines/cm$^2$ to $10^8$ lines/cm$^2$, we obtain the following values for the probable angular deviation:

$$\varphi_{\rho=10^6} \simeq 2.2' \qquad \varphi_{\rho=10^7} \simeq 13' \qquad \varphi_{\rho=10^8} \simeq 1°9'$$

When the full beam is employed, the reflection obtained comes from a region on the specimen along a line about 1 cm in length. We can readily detect horizontal deviations in the position of the reflection of about 1 min. and vertical deviations of about 10 min. In the absence of small angle boundaries, no horizontal deviations from the mean reflection position were observed that amounted to more than 1 or 2 minutes. No vertical deviations were detected. This indicates that either the dislocation densities of the specimens observed were of the order of $10^6$ lines/cm$^2$ or less, or that the tilting block model from which equation (2) is derived is not a good representation of the situation in a real crystal.

Variation of Line Width with Diffraction Angle: The results of the measurements made to determine the dependence of the line width on the diffraction angle are tabulated in Table 3 and summarized graphically in figures 4 and 5. It is not possible to decide from these graphs whether the data follows the tangent $\theta$ relation for strain broadening, or the secant $\theta$ relation for particle size broadening. The results obtained on the quartz are

somewhat indefinite due to scatter in the points obtained. Dislocation densities calculated from the slopes of the curves in figures 4 and 5 are tabulated in Table 4 along with the values calculated from equation (2). The agreement between the dislocation densities estimated in the aluminum specimen by the tilting block model and the particle size relation is quite good.

The low dislocation densities obtained from the strain broadening relation as compared with the densities estimated from the tilting block model and from the particle size relation indicates that strains of the type considered in the derivation of equation (6) are quite small. The dislocation densities tabulated in Table 4 for particle size broadening are calculated under the assumption that strain broadening is negligible, and the strain broadening values assume that particle size broadening is negligible. If the value for dislocation densities given by the tilting block model and by the particle size broadening relation are accepted as the most reliable estimates of the dislocation density in the aluminum crystal examined, the low dislocation density obtained using the strain broadening relation can only be consistent with tilting block and particle size densities if the dilations present are much smaller than one would expect from most dislocation arrangements. It can be consistent if:

1. Screw type dislocations predominate in annealed crystals. This appears to be a reasonable possibility, since the strain energy of an edge type dislocation is about 50 per cent greater than that of a screw dislocation.

2. Edge type dislocations, when present in annealed
   crystals are in arrays which minimize the strain
   energy of the crystal. One dislocation array which
   is commonly observed in metal crystals is the small
   angle boundary.

Survey of Aluminum Single Crystals: Comparison of the
strain-anneal specimens (numbered series) with the melt-grown
specimens (alphabet series) from the survey results as tabulated
in Table 5 indicates that on the average the former show a
slightly better degree of crystal perfection. The rather
surprising aspect of this survey is that there were a number of
melt-grown specimens which were comparable in all respects to
the strain-anneal specimens. In general, the degree of crystal
perfection present in the melt-grown specimens is much better than
would be expected from information available in the literature.

In the melt-grown specimens, the number of small angle
boundaries intercepted by the beam was determined in part by the
angle the line of the focus made with the specimen axis. When
the focus was perpendicular to the specimen axis, it intercepted
on an average three times as many boundaries as when it was
parallel to the specimen axis. This indicates that the boundaries
tend to run parallel to the specimen axis (and the growth direction).
No indications of a preferred direction of the boundaries was
observed in the strain-anneal specimens.

The density of dislocations in the small angle boundaries
is comparatively small. For the strain-anneal specimens, the

average density of dislocations in boundaries is $6.2 \times 10^4$ lines/cm$^2$, and 'or the melt-grown specimens $1.4 \times 10^5$ lines/cm$^2$. The line widths of the strain-anneal specimens tend to be slightly smaller than those of the melt-grown specimens. Annealing of several melt-grown specimens produced no detectable changes in the line widths. The average corrected line widths for both groups of specimens are 0.62' for the melt specimens and 0.45' for the strain-anneal specimens. The latter value is about the same as observed for the $(2\bar{1}0)$ reflection from the quartz. The dislocation densities corresponding to these line widths are $6 \times 10^6$ lines/cm$^2$ for the melt specimens and $3.5 \times 10^5$ lines/cm$^2$ for the strain anneal specimens.

Some insight as to one of the sources of variation in line widths from specimen to specimen is given by a series of micro-photometer measurements of the (111) reflection from specimen D and the $(2\bar{1}0)$ reflection of the quartz. Each reflection was scanned at 0.5 cm intervals along its length over the central 5 cm of the line where the film density in the reflection was uniform. The root mean square deviation of the measurements from the aluminum specimen amounted to 20 per cent of the corrected line width, while the deviation for the quartz was 2 per cent. Close visual examination of the aluminum lines indicated that small bulges were present on the lines (compare a and b in figure 2). Some, but not all of the melt-grown specimens gave reflections with this type of variation in the lines, whereas the strain-anneal specimens rarely showed this type of variation. These variations

are thought to correspond to small angle boundaries which are not resolved and represent angular disorientations of less than about 20" of arc.

The comparable degree of perfection observed in the quartz and aluminum specimens is consistent with previous work which employed this x-ray method.[2] Comparison of our results, which were obtained by reflection, with previous results obtained in transmission[2] do not indicate any sensible differences in the degree of crystal perfection observed. This point is of some importance, since the reflection method "sees" only a thin layer at the surface and the question naturally arises as to whether these surface observations are also applicable to the interior of the crystal. In that the transmission measurements mentioned above were made on 0.5 mm thick specimens, it appears that our measurements in reflection are representative of the material to a depth comparable to this.

The unexpected high degree of crystal perfection in the melt-grown specimens is probably associated with the crystal growing method employed. No attempt has been made to date to ascertain which of several possible factors are of importance. The factors that are different in the "soft-mold" method from more conventional methods are the strength (or softness) and the radial thermal insulation provided by the mold material. The softness of the mold material reduces the possibility of strain due to differential thermal contraction in specimens "keyed" in the mold, and in addition, permits easy removal without the danger of accidentally

damaging a specimen. The radial thermal insulation provided by
the mold material combined with extraction of heat by conduction
from the bottom of the mold favors a truly axial heat flow in
the specimen during solidification. This last factor is thought
to be the more important of those discussed.

## CONCLUSIONS

The use of high resolution x-ray diffraction methods on
annealed crystals offers good possibilities of obtaining consider-
able information about the dislocation densities and distributions.
The present work indicates that in annealed aluminum single
crystals, the majority of the dislocations are present in
essentially random arrays and in densities of about $10^6$ lines/cm$^2$.
Small angle boundaries contribute but little to the overall
dislocation density, contributing on the average about $10^4$ to $10^5$
lines/cm$^2$.

No basic differences were observed between aluminum single
crystals prepared by the strain anneal method and those grown from
the melt. The major difference between the two types of crystals
is that on the average the number and angular range of small angle
boundaries is less in the strain anneal crystals.

Additional work is needed to confirm and expand the results
of this investigation. Extension of the work on the statistics
of dislocation distributions--both experimental and theoretical--
is particularly desirable. Experimental techniques different
from those employed in this work should be investigated.

## ACKNOWLEDGEMENT

# REFERENCES

1. Guinier, A. and Tennevin, J. Acta Crystallographica, **2**, p. 133, 1949.

2. Lambot, H., Vassamillet, L., and Dejace, J., Acta Metallurgica, **1**, p. 711, 1953.

3. Gay, P., Hirsch, P.B., and Kelly, A., Acta Metallurgica, **1**, p. 315, 1953.

4. Darwin, C. G., Philosophical Magazine, **27**, pp. 315 and 675, 1914.

5. Cottrell, A. H., _Dislocations and Plastic Flow in Crystals_ (a) 100, (b) 40 Oxford University Press, London, 1953.

6. Guinier, A., _Imperfections in Nearly Perfect Crystals_ p. 402, John Wiley and Sons, 1952.

7. Schwope, A. D., Shober, F. R., and Jackson, L. R., Creep In Metals. NACA TN 2618, 1952.

8. Noggle, T. S., Rev. Sci. Inst. **24** p. 184, 1953.

9. Beck, P. A., Kremer, J. C., Demer, L. J., and Holzworth, M. L., Trans. AIME **175** p. 372, 1948.

## TABLE I

| | |
|---|---|
| Separation of $K\alpha_1$ and $K\alpha_2$ | .085 mm |
| Width of $K\alpha_1$ at one-half maximum intensity | .068 mm |
| Width of $K\alpha_2$ at one-half maximum intensity | .058 mm |
| Full width at background intensity level | .20 mm |
| Vertical height | 10 mm |
| Horizontal angular aperture . . . approximately | $1°$ |
| Vertical angular aperture . . . approximately | $3/4°$ |

## TABLE II

### Line Widths in Minutes

| Specimen | Aperture Slit Height mm | $\alpha_1$ Experimental Width* | $\alpha_1$ Corrected For Spectral Width | $\alpha_2$ Experimental Width* | $\alpha_2$ Corrected For Spectral Width | Average Corrected Width |
|---|---|---|---|---|---|---|
| Aluminum | 0.1 | 1.72 | 1.27 | 1.42 | .82 | 1.04 |
| D | 0.2 | 1.10 | .65 | 1.08 | .48 | .56 |
| | 0.5 | 1.07 | .62 | 1.01 | .41 | .52 |
| (111) | 1.0 | 1.23 | .78 | 1.33 | .73 | .76 |
| Reflection | 2.0 | 1.08 | .63 | 1.05 | .45 | .54 |
| | 5.0 | 1.29 | .84 | 1.23 | .63 | .74 |
| Quartz | 0.1 | 1.28 | .83 | 1.15 | .55 | .69 |
| $(2\bar{1}0)$ | 0.2 | .95 | .50 | .93 | .33 | .42 |
| | 0.5 | .93 | .48 | .95 | .35 | .42 |
| Reflection | 1.0 | 1.08 | .63 | 1.15 | .55 | .59 |
| | 2.0 | 1.07 | .62 | 1.23 | .63 | .62 |
| | 5.0 | 1.09 | .64 | 1.21 | .61 | .62 |

\* Average of three microphotometer scannings on the lines.

## TABLE XII

| Specimen and Reflection | Average Line Widths in Minutes | | | | |
|---|---|---|---|---|---|
| | Experimental Width | | Corrected* Width | | Average Corrected Width |
| | $a_1$ | $a_2$ | $a_1$ | $a_2$ | |
| **Aluminum Specimen D** | | | | | |
| (111) | 1.32 | 1.38 | .83 | .74 | .78 |
| (220) | 2.09 | 1.65 | 1.21 | .49 | .84 |
| (222) | 2.15 | 2.26 | .93 | .66 | .79 |
| (331) | 2.88 | 3.12 | .86 | .45 | .66 |
| (422) | 4.82 | 5.44 | 1.26 | .70 | .98 |
| (333) | 11.16 | 14.30 | 2.16 | 1.04 | 1.60 |
| **Quarts** | | | | | |
| (210) | 1.08 | 1.09 | .59 | .45 | .52 |
| (4$\bar{1}$0) | 1.50 | 1.80 | .29 | .20 | .24 |
| (5$\bar{2}$4) | 7.36 | 8.5 | 1.16 | .04 | .60 |

\* Corrected for spectral width and vertical aperture.
See Reference 2.

## TABLE IV

| Specimen | Dislocation Densities | | | |
|---|---|---|---|---|
| | Tilting | Block | Particle size | Strain |
| | I | II | | |
| Aluminum D | $6.2 \times 10^6$ | $1.18 \times 10^6$ | $8.6 \times 10^6$ | $1.5 \times 10^4$ |
| Quarts | $3.8 \times 10^6$ | $6.9 \times 10^5$ | $2 \times 10^5 - 5 \times 10^6$ | $4 \times 10^2 - 1 \times 10^4$ |

I — L = $7.6 \times 10^{-3}$ cm = average width at the specimen

II — L = $1 \times 10^{-1}$ cm = effective vertical beam height at the specimen

## TABLE V

| Specimen | Reflection | Mean Line Widths Uncorrected α₁ | α₂ | Corrected for Spectral Width α₁ | α₂ | Avg. no. of Small angle boundaries* | Average Boundary Angle | Maximum Disorientation |
|---|---|---|---|---|---|---|---|---|
| 7 | 220 | 1.45 | 1.52 | .63 | .42 | 1.8 | 1.1' | 3.0' |
| 10 | 220 | 1.42 | 1.36 | .60 | .26 | 5.0 | 1.2' | 5.2' |
| 13 | 311 | 1.34 | 1.55 | .29 | .15 | 2.8 | 0.9' | 3.4' |
| 14 | 220 | 1.39 | 1.43 | .57 | .33 | 2.3 | 1.2' | 2.4' |
| 15 | 311 | 1.51 | 1.74 | .46 | .34 | 1.3 | 0.9' | 1.4' |
| 18 | 220 | 2.12 | 1.83 | 1.30 | .73 | 1.0 | 0.7' | 1.5' |
| 22 | 200 | 1.04 | 0.90 | .51 | .19 | 0 | --- | --- |
|  | 311 | 1.29 | 1.49 | .24 | .09 |  |  |  |
|  | 311 | 1.62 | 1.81 | .57 | .41 |  |  |  |
| D | 311 | 1.32 | 1.38 | .87 | .78 | .7 | .8' | 1.5' |
|  | 220 | 2.09 | 1.65 | 1.27 | .55 |  |  |  |
| B | 311 | 1.87 | 2.14 | .82 | .74 | 1.4 | .8' | .8' |
| F Annealed | 220 | 1.60 | 1.73 | .78 | .63 | 1.7 | 4.8' | 34.4' |
|  | 311 | 1.30 | 1.45 | .48 | .35 |  |  |  |
| H | 311 | 1.58 | 1.83 | .53 | .43 | .8 | 2.5' | 5.5' |
|  | 311 | 2.32 | 2.46 | 1.27 | 1.06 |  |  |  |
| L | 311 | 1.50 | 1.62 | .45 | .22 | 1.0 | 2.25' | 4.1' |
|  | 200 | 1.77 | 1.64 | 1.24 | .93 |  |  |  |
| M | 311 | 1.33 | 1.58 | .28 | .18 | .3 | .7' | .7' |
| N | 311 | 1.61 | 1.87 | .56 | .47 | 6.2 | 3.4' | 13.5' |
| P | 220 | 1.67 | 1.66 | .85 | .28 | 1.5 | 1.4 | 2.61' |
|  | 311 | 1.91 | 1.93 | .86 | .53 |  |  |  |
| Q | 311 | 1.99 | 2.02 | .94 | .62 | 3.0 | 1.72' | 5.16' |
| S | 220 | 1.63 | 1.65 | .81 | .55 | 4.5 | 1.7' | 14.4' |
| T | 200 | 1.12 | 1.10 | .59 | .39 | 1.4 | 2.8' | 7.4' |
| V | 220 | 1.22 | 1.36 | .40 | .20 | 2.2 | 1.8' | 7.4' |
|  | 220 | 2.18 | 2.10 | 1.13 | 1.00 |  |  |  |
| PCI | 311 | 1.63 | 1.55 | .58 | .15 | 2.0 | 1.6' | 5.2' |
|  | 220 | 1.75 | 1.66 | .93 | .56 |  |  |  |
|  | 311 | 2.10 | 2.16 | 1.05 | .76 |  |  |  |

* These values are obtained by counting the discontinuities on each of the films obtained from a given specimen and dividing this count by the number of films. This gives approximately the average number of small angle boundaries that would be intersected by a line on a crystal 1 cm in length.
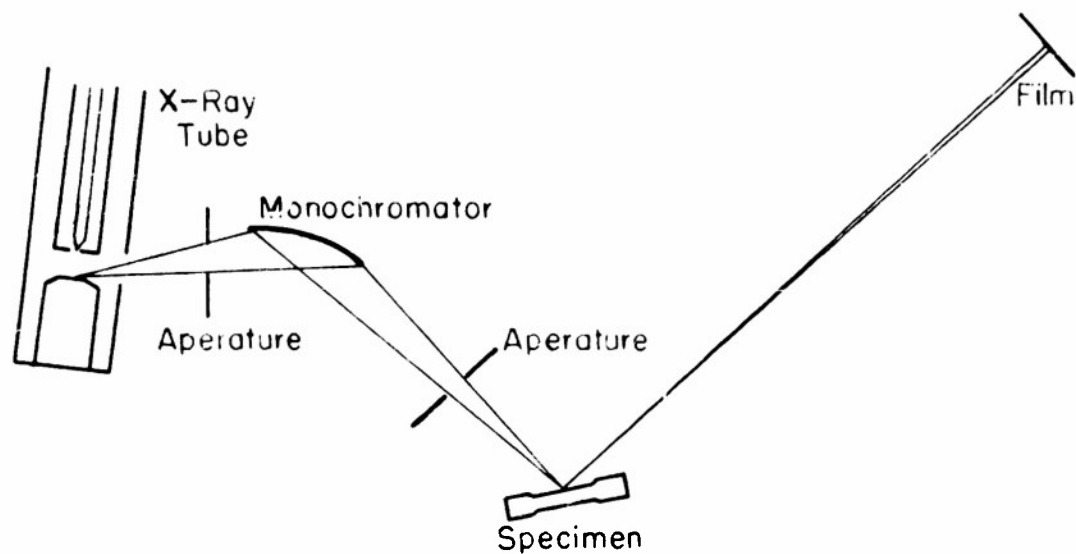
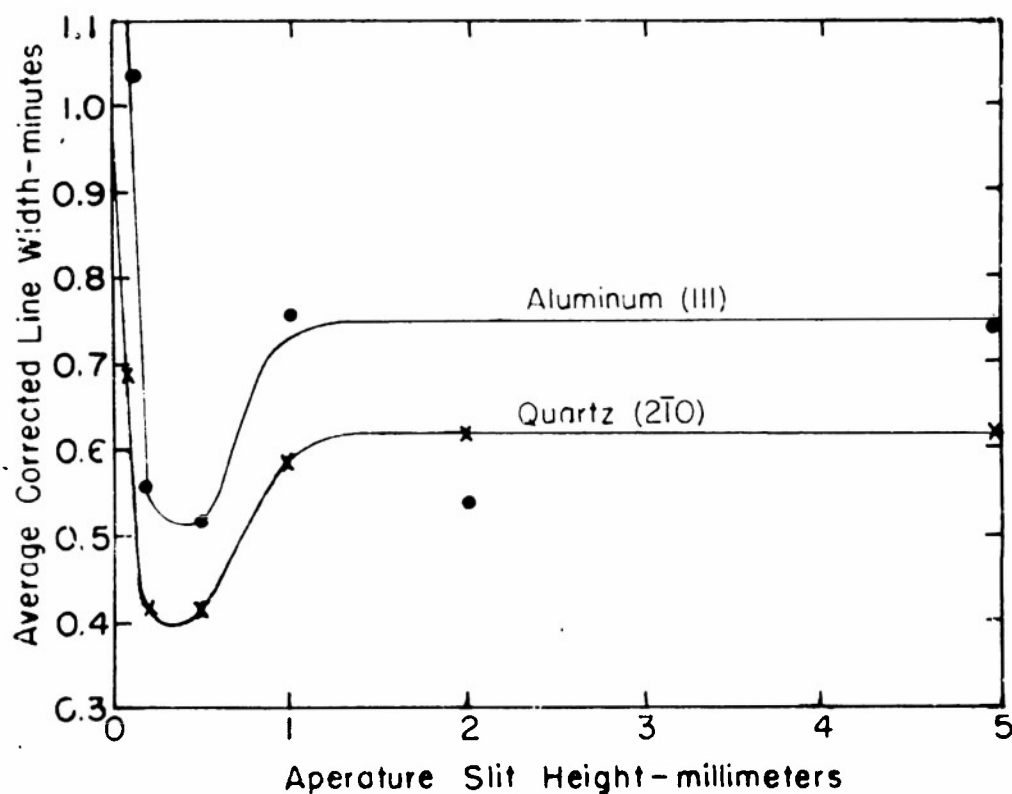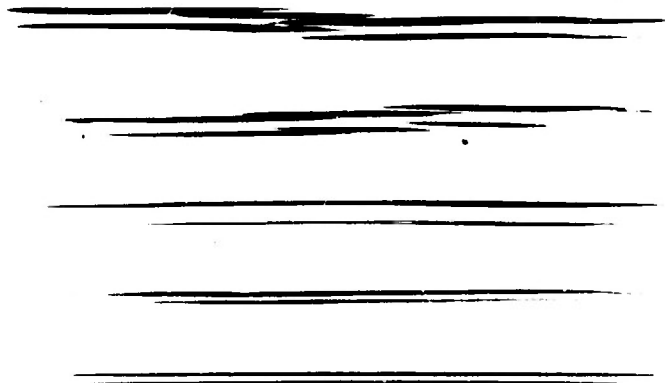Fig. I
Schematic Diagram of Experimental Set-up



Fig. 4

Effect of Aperoturing on the line widths of the (III) reflection
from Aluminum and the (2$\overline{1}$0) reflection from Quartz.
Cu. K$\alpha$ Radiation

Figure 1. Typical Microphotometer record obtained from films.



a  b  c  d  e

Figure 2. a. Quartz (2Ī0); b. Al. specimen D(111); c. Al. specimen 18 (311); d. Al. specimen 10(220); e. Al. specimen 5 (220). (Numbered specimens obtained by strain anneal, lettered specimens from the melt).
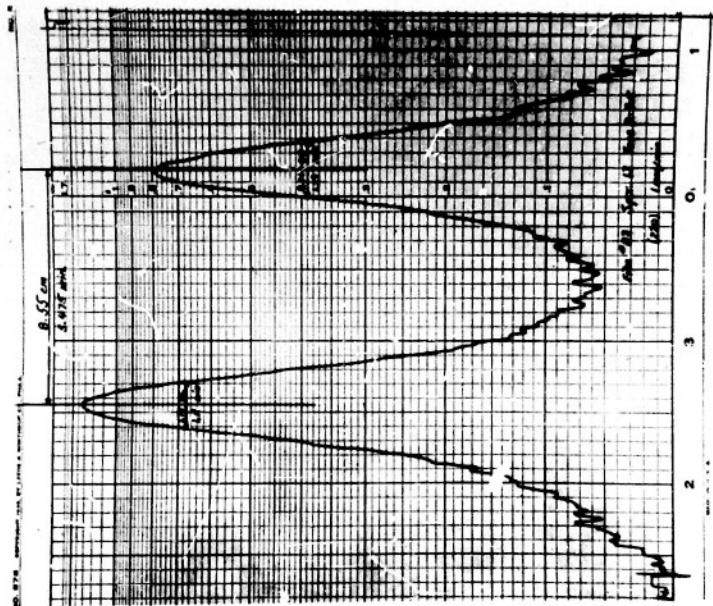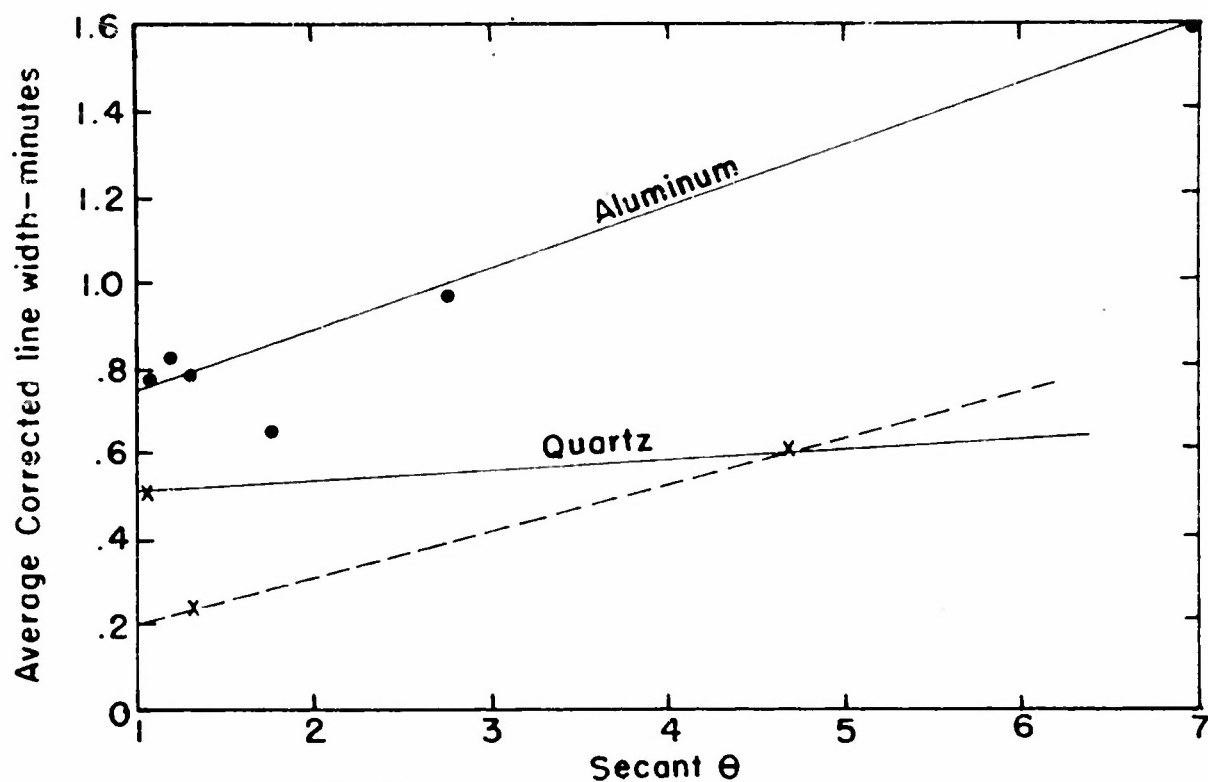
Fig. 5
Variations in line widths as a function of Secant Θ
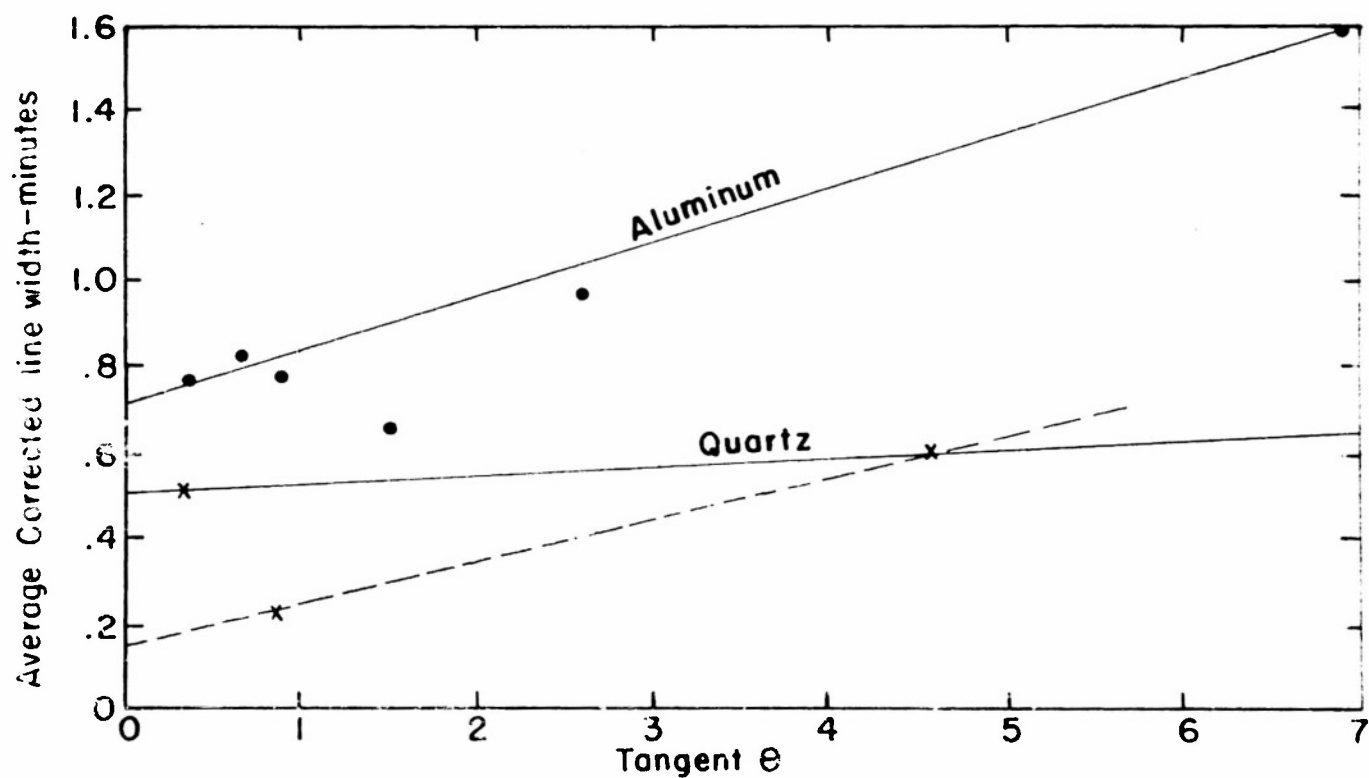


Fig. 6
Variations in line widths as a function of Tangent Θ

## DISTRIBUTION LIST

for

N6 ori  071 (54)

A. Government Distribution

1. Department of Defense

>Research and Development Board
>Information Office Library Branch
>Pentagon Bldg.
>Washington 25, D. C. (2 copies)

>Armed Services Technical Information Agency
>U. B. Bldg.
>Dayton 2, Ohio  (5 copies)

2. Department of the Navy

>Chief, Bureau of Aeronautics
>TD-4
>Navy Department
>Washington 25, D. C.

>Chief, Bureau of Ordnance
>Rea
>Navy Department
>Washington 25, D. C.

>Chief, Bureau of Ships
>Code 300
>Navy Department
>Washington 25, D. C.

>Chief of Naval Research
>Office of Naval Research
>Washington 25, D. C.
>Attn:  Physics Branch (Code 421)  (3 copies)

>Director
>Naval Research Laboratory
>Technical Information Officer (Code 2000) (9 copies)
>Code 2021 (2 copies)
>Washington 20, D. C.

>Director
>Office of Naval Research Branch Office
>150 Causeway Street
>Boston 14, Massachusetts

Director
Office of Naval Research Branch Office
346 Broadway
New York 13, New York

Director
Office of Naval Research Branch Office
86 East Randolph Street
Chicago 13, Illinois

Director
Office of Naval Research Branch Office
100 Geary Street
San Francisco 9, California

Director
Office of Naval Research Branch Office
1031 East Green Street
Pasadena 1, California

Officer in Charge
Office of Naval Research London Branch Office
Navy No. 100
Fleet Post Office
New York, New York (2 copies)

Physics Department
Post Graduate School
U. S. Naval Academy
Annapolis, Maryland

Librarian
U. S. Naval Post Graduate School
Monterey, California

U. S. Naval Electronics Laboratory Library
San Diego 52, California

Director
Physics Research
Naval Ordnance Laboratory
White Oaks, Maryland

Director
Physics Research
Naval Ordnance Test Station
Inyokern
China Lake, California

3. Department of the Air Force

  Commanding General
  Air Research and Development Command
  Attn: Office of Scientific Research
  Post Office Box 1395
  Baltimore 3, Maryland (2 copies)

  Air Adjutant General
  Mail and Receiving Management Division
  Headquarters, U.S.A.F.
  Washington 25, D. C.

4. Department of the Army

  Commanding Officer
  Engineering Research and Development Laboratories
  Fort Belvoir, Virginia
  Attn: Technical Intelligence Branch

  Office of Ordnance Research
  Box CM, Duke Station
  Durham, North Carolina (2 copies)

  Signal Corps Engineering Laboratory
  Fort Monmouth, New Jersey
  Attn: Technical Information Officer

5. Department of Commerce

  Office of Technical Services
  Technical Reports Section
  Department of Commerce
  Washington 25, D. C. (2 copies)

  Director
  National Bureau of Standards
  Washington 25, D. C. (2 copies)

  Director
  National Bureau of Standards
  Corona, California

6. Other Agencies

  National Research Council
  Division of Physical Sciences
  National Academy of Sciences
  Washington, D. C.

  Director
  National Science Foundation
  Washington 25, D. C.

  U. S. Atomic Energy Commission
  Technical Information Service
  P. O. Box 62
  Oak Ridge, Tennessee

# Armed Services Technical Information Agency

Because of our limited supply, you are requested to return this copy WHEN IT HAS SERVED YOUR PURPOSE so that it may be made available to other requesters. Your cooperation will be appreciated.

# AD 43390

Reproduced by

# DOCUMENT SERVICE CENTER
## KNOTT BUILDING, DAYTON, 2, OHIO

# UNCLASSIFIED